K03/2

Prediction of Strong Ground Motion Using a Semi-Empirical Technique

Katsuhiro KAMAE, Kojiro IRIKURA
Kyoto University, Kyoto, Japan
Yasunaga FUKUCHI
Nogoya Institute of Technology, Nagoya, Japan

ABSTRACT

We propose a synthetic procedure for predicting strong ground motion at a specific site from a future large earthquake using a semi-empirical method. First of all, we estimate regional scaling relations of source parameters based on observed ground motion data from earthquakes occurring in the objective region. We construct a large earthquake by a superposition of many small-events based on the scaling law of earthquakes. We use either the observed records or the artificially simulated motions for small-events as Green's functions. The synthetic procedure in the former case (the so-called empirical Green's function method) is written by Kamae et al (1990). In this paper, we present mainly the synthetic procedure in the latter case, i.e., the simulation of artificial ground motion based on a semi-empirical method and the synthesis results using that as semi-empirical Green's function. Boore (1983) proposed a simple method to simulate a high-frequency ground motion based on seismological spectral model. We apply his method to simulate small-event motions from sub-faults. The simulated ground motions are used as Green's functions modified by site effects evaluated theoretically from geologic structures and by path effects such as attenuation and broadening of waveform envelope empirically in the objective region. Finally, we attempt to predict the strong ground motion due to a future large earthquake ($M7, \Delta=13$km) using the same summation procedure as the former case. We obtained the results that the synthetic motions are in reasonable agreement with those in the former case.

1 INTRODUCTION

A semi-empirical method to simulate strong ground motions using small-event motions as empirical Green's functions is one of the most effective techniques to estimate the input motion for the earthquake resistant design of a structure. Since Hartzell's pioneering study (1978), many researchers have applied this method to simulating strong ground motions due to a main event using records for small-events such as aftershocks. Kamae et al (1990) proposed a synthetic procedure for predicting strong ground motion at a specific site from a future large earthquake using the records of the actual small-events as empirical Green's functions (the so-called empirical Green's function method). First of all, we estimate regional scaling relations of source parameters based on the earthquake observation in the objective region. According to the scaling law of earthquakes, we construct a large earthquake by a superposition of small-events radiated from many sub-faults.

It is important to study how to apply this method in case of having no appropriate observation records in the objective site. In this paper, we present mainly the simulation of artificial small-event motion at a specific site based on a semi-empirical method, and the prediction of the strong ground motion using artificial small-event motion as semi-empirical Green's function. Here, we use the same summation procedure as the empirical Green's function method.

SMiRT 11 Transactions Vol. K (August 1991) Tokyo, Japan, © 1991

2 SYNTHESIS METHOD

In the case that both large and small events have the ω^{-2} spectral characteristics, the synthesis formulation is according to Irikura (1983,1986).

$$U(t) = \sum_{i=1}^{N}\sum_{j=1}^{N} \frac{r}{r_{ij}} F(t - t_{ij}) * u(t) \ , \qquad t_{ij} = \frac{(r_{ij}-r_0)}{\beta} + \frac{\xi_{ij}}{V_R} \qquad (1)$$

where $U(t)$ and $u(t)$ are synthetic motion for large earthquake and small-event motion, respectively. r is the hypocentral distance of the small-event, r_{ij} is that of the (i,j) sub-fault divided into $i \times j$ divisions on the large fault plane, r_0 is the distance between the starting point and the observation site, and ξ_{ij} is the distance between the starting point and the (i,j) sub-fault. β is the shear wave velocity, V_R is the rupture velocity. $F(t)$ is given as follows:

$$F(t) = \delta(t) + \frac{1}{n'} \sum_{k=1}^{(N-1)n'} \delta[t-(k-1)\frac{\tau}{(N-1)n'}] \qquad (2)$$

where n' is arbitrary number, τ is the rise time of the large earthquake. The seismic moment ratio of large earthquake to small one should be equal to N^3 if the self-similar scaling is ideally applicable.

As shown in an earlier study (Kamae et al, 1990), the small-event motion $u(t)$ is corrected to be an empirical Green's function appropriate for each sub-fault by considering the differences in stress drop, attenuation effect due to propagation media, high-frequency cutoff (F_{max}) of acceleration spectra, and radiation patterns between large and small events.

3 STOCHASTIC SIMULATION OF SMALL-EVENT MOTION

In this section, we artificially simulate the small-event motions, including the site effects evaluated theoretically from geologic structures and path effects such as attenuation and broadening of waveform envelope empirically in the objective region.

Boore (1983) proposed a simple method to simulate high-frequency ground motions based on a seismological spectral model. His idea is to generate a stochastic time series of filtered and windowed Gaussian white noise whose acceleration amplitude spectrum is matched, on the average, to an ω-squared spectrum with a high-frequency cutoff (F_{max}). Although he considers the seismological spectral model, the physical characteristics of the fault, such as size, slip and rupture propagation, are not taken into account. Therefore, it is not valid to apply this method to predictions of motions close to large earthquakes, which are strongly influenced by the spacial extent of slip and rupture propagation (directivity) on the fault plane. In this paper, we apply his method to simulate the motion for a small-event because its size is small and the effect of rupture propagation is negligible. Following Boore (1983), it starts with the windowing of a time sequence of band-limited random white Gaussian noise with an expected mean of zero and variance chosen to give unit spectral amplitude on the average. Next, the spectrum of the windowed time series is multiplied by the specified spectrum. Finally, transformation back to the time domain results in a final transient time series. Here, he adopted the Brune (1970) spectrum modified to remove frequencies above a certain cutoff frequency for the specified spectrum. The acceleration spectrum $A(\omega)$ of shear waves at a distance R from a fault with seismic moment M_0 is

$$A(\omega) = C\, M_0\, S(\omega,\omega_c)\, P(\omega,\omega_m) \frac{e^{\frac{-\omega R}{2Q\beta}}}{R} \ , \qquad C = \frac{R_{\theta\phi} \cdot FS \cdot PRTITN}{4\pi\rho\beta^3} \qquad (3)$$

$R_{\theta\phi}$ is the radiation pattern, FS is the amplification due to the free surface, $PRTITN$ is the reduction factor that accounts for the partitioning of energy into two horizontal components, and ρ and β are the density and shear wave velocity, respectively. The source spectrum S is given by formula (4). The high-cut filter P is assumed to be formula (5) in the present paper.

$$S(\omega,\omega_c) = \frac{\omega^2}{1 + (\frac{\omega}{\omega_c})^2} \qquad (4)$$

$$P(\omega,\omega_m) = \frac{1}{1 + (\frac{\omega}{\omega_m})^n} \qquad (5)$$

where ω_c is the corner angular frequency. n equals to 1, and F_{max} ($=\omega_m/2\pi$) depends empirically on the seismic moment as shown by

$$F_{max} = 7.31 \times 10^3 M_0^{-0.12} \qquad (6)$$

according to Faccioli (1986). We have already shown the validity of adopting this relation by Kamae et al (1990).

As we have seen, the specified spectrum $A(\omega)$ is controlled by two parameters : seismic moment M_0 and corner frequency ($f_c=\omega_c/2\pi$). These two source parameters have been related through the following regional scaling relation based on ground motion data of six earthquakes with magnitudes of more than 4 occurring in the objective region.

$$\log M_0 = -3.0 \log f_c + 23.8 \qquad (7)$$

Consequently, we can specify the spectrum by only one parameter- seismic moment. Changing f_c for the fault area (S) using Sato and Hirasawa' formula, formula (7) becomes

$$\log M_0 = 1.5 \log S + 23.0 \qquad (8)$$

Furthermore seismic moment is empirically related to magnitude (by JMA) as shown by

$$\log M_0 = 1.33\ M + 17.0 \qquad (9)$$

Next, we use a shaping window whose length is controlled by the empirical relation between duration time (T_D) and magnitude (M) obtained from the earthquake observation. Because the simulated ground motion must include the regional path effects such as attenuation and broadening of waveform envelope. The regional relation between T_D and M is approximately consistent with the following empirical formula (10) obtained by Hisada and Ando (1976) as shown in Fig.1.

$$\log T_D = 0.31\ M - 0.77 \qquad (10)$$

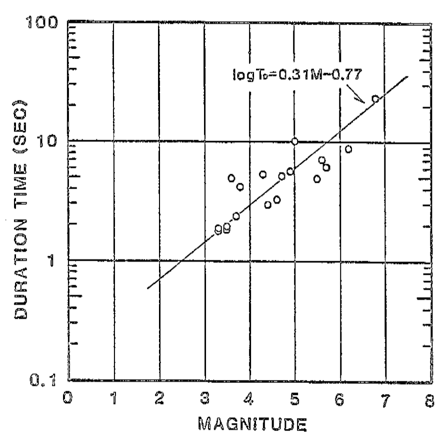

Fig. 1 Duration times versus Magnitude (by JMA) for earthquake occurring in the objective region.

According to above procedure, we simulated the ground motions at several distances (R=10km,20km,30km and 60km) from faults with several magnitudes (M=3,4 and 5). The other parameters needed in the simulation were taken to be : ρ=2.7 g/cm^3 ; β=3.6 km/sec, $R_{\theta\phi}$=0.63, $Q=110\sqrt{f}$ (the empirical relation in the *Kinki* district, *Japan*, obtained by Akamatsu, 1980 : f is a frequency), FS=2 and $PRTITN$=0.71.

The mean peak accelerations and peak velocities from the 20 motions generated by simply changing the seed of the pseudo-random number generator are shown in Fig-2, along with the peak accelerations and peak velocities (calculated by integration of the accelerograms) from data recorded on the outcropping rock site for earthquakes with magnitudes from 3 to 5. The peak accelerations and peak velocities from the simulations are in reasonable agreement with observed data in the range R=20 km to R=30 km. Here the discrepancies at greater hypocentral distances may be caused by considering only the shear wave contribution to the simulated ground motions.

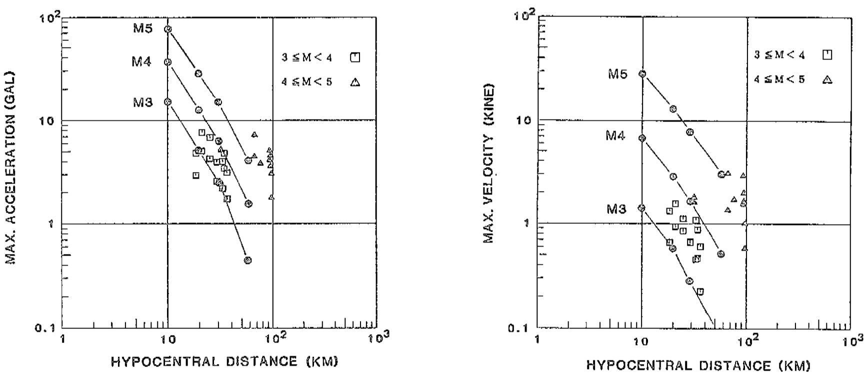

Fig. 2 Comparison of peak accelerations and velocities from data on the outcropping rock site (symbols □ and △) and those derived from 20 simulations (closed circles).

4 SYNTHESIS OF LARGE EARTHQUAKE WITH M7

In this section, we attempt to predict the strong ground motion from a future large earthquake ($M7, \Delta=13$km) using the small-event motion simulated in the preceding section as semi-empirical Green's function. The locations of the fault and the observation site are shown in Fig.3. The epicenter of an actual small-event (*M4.4*) used as empirical Green's function in Kamae et al (1990) is also shown by symbol (☆) in the figure. The resulting synthesis using the record of this actual small-event is referred to to verify the validity of the synthesis procedure proposed in this paper. Now we select the appropriate one as the semi-empirical Green's function from the 20 simulated ground motions by checking if these Fourier amplitude spectra are in reasonable agreement with the desired spectrum. The selected ground motion is modified as the peak acceleration is consistent with the average of the 20 simulations.

Using two simulated motions (*M4* and *M5* at R=20km) individually, we have synthesized the strong ground motion for the future large earthquake (*M7*) caused by the *NEGORO* fault in *Wakayama, Japan.* The source parameters of the target event and two simulated events are summarized in Table 1 and Table 2, respectively.

5 SYNTHESIS RESULTS AND DISCUSSION

The synthetic acceleration motions of horizontal component in the observation site are shown in Fig.4 , together with simulated motions and the actual small-event motion used as Green's functions. The resultant motions are synthesized according to the procedure proposed by Kamae et al (1990). The peak accelerations, peak velocities and duration times of the synthetic motions are summarized in Table 3, along with those of the synthetic motion using the actual small-event

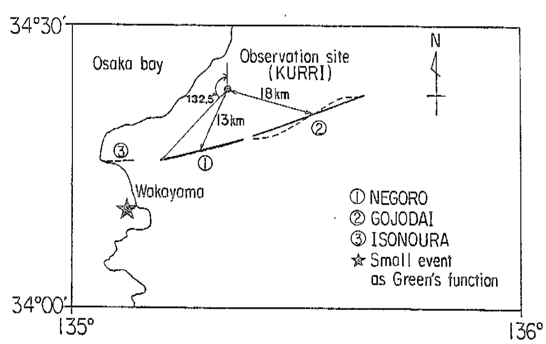

Fig. 3 Locations of observation site, the *NEGORO* fault and actual small-event.

Table 1 Source parameters for the target earthquake.

Strike	N77.6°E
Slip type	Strike slip
Dip angle (degree)	90
Length (km)	20
Width (km)	10
Depth (top of the fault) (km)	0
Seismic moment (dyne·cm)	3.34×10^{26}
Rise time (sec)	1.6
Stress drop (bar)	276
Rupture vel. (km/sec)	2.5
Shear wave vel. (km/sec)	3.6

Table 2 Source parameters for the simulated small earthquake.

M	R (km)	M_0 (dyne·cm)	S (km^2)	α
4	20	0.242×10^{23}	0.35	1.0
5	20	0.334×10^{24}	2.0	1.0

α : The ratio large event's stress drop to small event's

motion. Furthermore, these synthetic velocity response spectra are shown in Fig.5. The synthetic motion using simulated motion for *M4* tend to be slightly underestimated in the maximum peak, compared with those using that for *M5*, although the waveform envelopes are similar to each other and both velocity response spectra show good agreement in absolute amplitude at periods shorter than about 1 sec. All the characteristics of synthetic motion using simulated motion for *M5* are in reasonable agreement with those using the actual small-event motion.

Table 3 Peak accelerations, peak velocities and duration times of synthetic motions.

Small event	Maximum peak: Acceleration (gal)	Maximum peak: Velocity (kine)	Duration time (sec)
M4	299.3	12.9	3.5
M5	391.4	17.7	4.9
M4.4	412.2	21.5	5.7

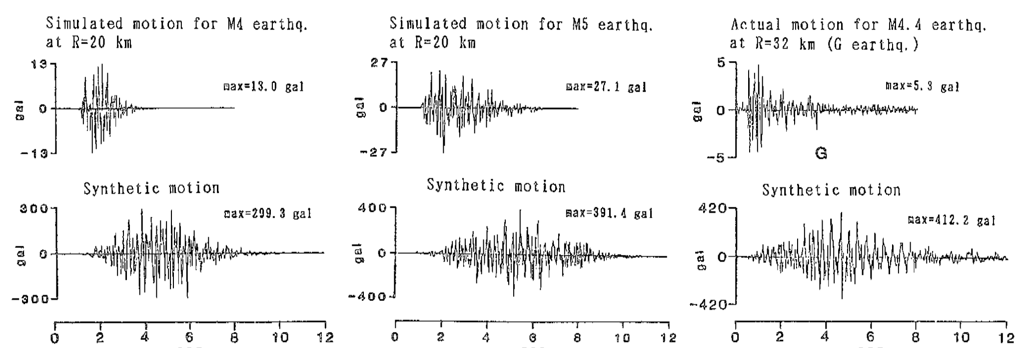

Fig. 4 Small-event motions and synthetic motions. Left : Simulated motion for *M4* earthquake at R=20 km and synthetic motion using that. Center : Simulated motion for *M5* earthquake at R=20 km and synthetic motion using that. Right : Actual motion for *M4.4* earthquake at R=32 km and synthetic motion using that.

6 CONCLUSIONS

A synthetic procedure has been proposed to predict strong ground motions using artificially simulated small-event motions as substitute for the actual motions. The essence of the method is (1) to simulate the small-event motions, including the site effects and path effects such as attenuation and empirical broadening of waveform envelope in the objective region, based on the stochastic simulation method proposed by Boore (1983), and (2) to synthesize the strong ground motion accompanying a large earthquake ($M7, \Delta=13$km) using two simulated small-event motions for $M4$ and $M5$ earthquakes at a distance R=20km as semi-empirical Green's function. We obtained the results for which the characteristics of the synthetic motion using simulated motion for $M5$ were in good agreement with those predicted by the empirical Green's function method. Therefore, in cases where no suitable records of actual small-events are available, we can predict strong ground motions by means of the synthetic procedure presented in this paper.

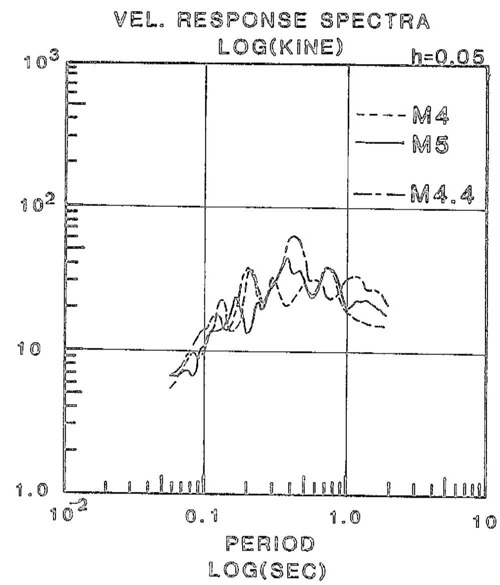

Fig. 5 Velocity response spectra for synthetic motions.

REFERENCES

Hartzell, S. (1978). Earthquake aftershocks as Green's functions, J. Geophys. Res. Letters, Vol.5, pp.1-4.

Kamae, K., K. Irikura and Y. Fukuchi (1990). A study of ground motion prediction procedure using empirical Green's function, Proc. 8th Japan Earthq. Eng. Symp., pp.223-228.

Irikura, K. (1983). Semi-empirical estimation of strong ground motion during large earthquake, Bull. Disas. Prev. Res. Inst., Kyoto Univ., Vol.33, pp.63-104.

Irikura, K. (1986). Prediction of strong acceleration motion using empirical Green's function, Proc. 7th Japan Earthq. Eng. Symp., pp.151-156.

Boore, D. M. (1983). Stochastic simulation of high-frequency ground motions based on seismological models of the radiated spectra, Bull. Seism. Soc. Am., Vol.73, No.6, pp.1865-1894.

Brune, J. N. (1970). Tectonic stress and the spectra of seismic shear waves from earthquakes, J. Geophys. Res., Vol.75, pp.4997-5009.

Sato, T. and T. Hirasawa (1973). Body wave spectra from propagating shear cracks, J. Phys. Earth, Vol.21, pp.415-431.

Hisada, T. and H. Ando (1976). Relation between duration of earthquake ground motion and the magnitude, Kajima Institute of Construction Technology.

Akamatsu, J. (1980). Attenuation property of seismic waves and source characteristics of small earthquake, Bull. Disas. Prev. Res. Inst., Kyoto Univ., Vol.30, pp.53-80.